Revisited Mass-Radius relations for exoplanets below 120M⊕

J. F. Otegi[1,2], F. Bouchy[2], R. Helled[1] & C. Dorn[1]

University of Zurich[1] & University of Geneva[2]

Introduction

The Kepler mission has clearly impacted the field with the detection of more than 2300 exoplanets. For many of the Kepler exoplanets, radial velocity follow-up is restricted to a small fraction corresponding to the brightest host stars. As a result, in order to characterise the exoplanets researchers often rely on a theoretical mass-radius (hereafter M-R) relation.

We present an updated exoplanet catalog based on reliable, robust and as much as possible accurate mass and radius measurements of transiting planets up to 120 $M_\oplus$. In this poster we show the following:

- The selection criteria that we follow in order to build a "reliable and updated" exoplanet catalog.
- The analysis of the revisited M-R diagram. We explore the demography, derive new M-R relations and look for dependences with other parameters.
- Determining the internal structure is extremely challenging due to the intrinsic degeneracy as several compositions lead to the same mass and radius. We discuss several aspects that affect internal structure characterisation.

Exoplanet selection

These are some of the main criteria we used to build a "reliable and updated" catalog:

- We select the data from the NASA Exoplanet Archive on July 2019 for planets with masses up to 120M⊕ and filter the data to consider only exoplanets with measurement uncertainties smaller than σ/M = 25% and σ/R = 8%.
- We discard the mass determinations inferred by Stassun et al. (2017), where the host star masses and radii were replaced by the value derived from GAIA photometry and with uncertainties clearly overestimated.
- In some cases Marcy et al. (2014) gives an estimate of the planetary masses for single transiting planet with weak level of validation/confirmation.
- We rely on the robustness criterion for TTVs presented in Hadden & Lithwick (2017), and discard the unreliable TTVs mass determination.
- We update some mass measurements to the ones presented in more recent publications and we include several exoplanets that are missing in the NASA Exoplanet archive.

Analysis of the revisited M-R diagram

Two distinct exoplanet populations

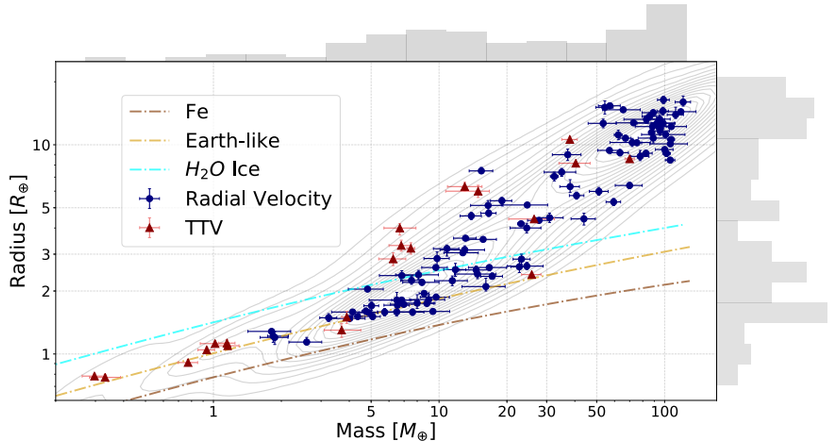

Figure 1: Revisited M-R diagram. The red triangles and blue circles correspond to data with mass determination from TTVs and RVs, respectively. We also display the composition lines of pure-iron (brown), Earth-like planets (light-brown) and water ice (blue) (Dorn et al 2015).

The resulting M-R diagram shows two distinct exoplanet populations: one of them closely follows an Earth-like composition, and a second one corresponds to a more volatile-rich composition. The rocky exoplanet population shows a relatively small density variability and ends at a mass of 25 $M_\oplus$., possibly indicating the maximum core mass that can be formed.

The Mass-Radius Relation

Since the two exoplanet populations overlap in mass and radius, we use the pure-water composition line to separate the rocky and volatile-rich regimes and fit both populations. The coefficients we get are rather insensitive to the used water EOS and the limits on mass and radius uncertainties chosen for the catalog.

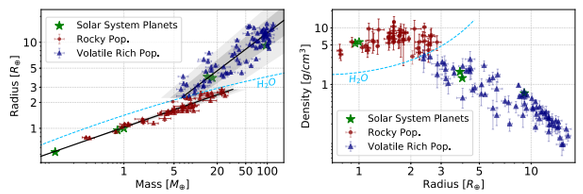

Figure 2: Density against radius (left) and M-R diagram (right) with the rocky population and the volatile-rich population separated by pure-water composition line. The right panel shows the fitted M-R relations.

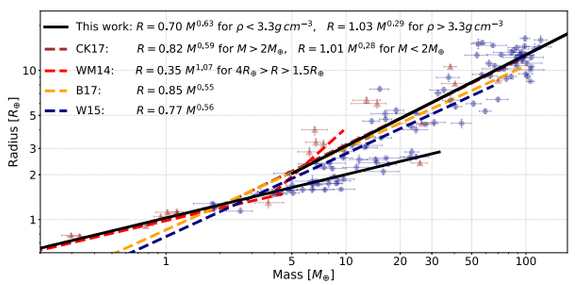

Figure 3: Comparison of the M-R relations in the literature with the one obtained from our revisited catalog. The analytic expressions of the M-R relations CK17, WM14, B17 and W15 correspond to Cheng & Kipping (2017), Weiss & Marcy (2014), Bashi et al. (2017) and Wolfgang et al. (2015).

Our M-R relation is similar to the one inferred by Cheng & Kipping (2017), but the transition from the rocky to the volatile-rich regime is defined for a mass of 2$M_\oplus$, so they underestimate the masses of most of the rocky exoplanet population. We see that single and unique relation for all the planets and do not represent the rocky population correctly, as used in Wofgang et al. (2015) and Bashi et al. (2017)

BONUS Constraining planetary interiors

We use the internal structure model presented in Dorn et al. 2017 with a full Bayesian analysis based on a Nested Sampling scheme to quantify the degeneracy and to produce the posterior probability distributions of the internal structure parameters. We use it to discuss several aspects that affect internal characterisation.

Dependence of internal structure determination on observational uncertainties

The Shannon entropy H (Tarantola 1987) compares the prior and posterior distributions of the parameters and estimates the amount of information carried by the data. In Figure 4 we show the variation of the Shannon entropy with the mass uncertainty for different internal parameters and planets of different mass and radii. The colorbar indicates how much an observational improvement allows to better constrain the internal parameter.

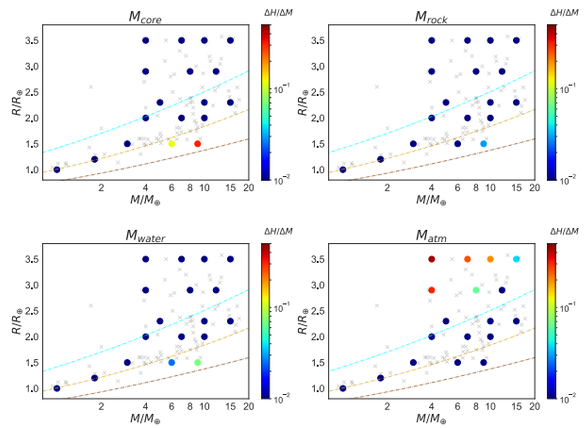

Figure 4: Slopes of the linear fit of the Shannon entropy against the width of the observational mass uncertainty for varios model parameters and synthetic planets.

At high and low planetary bulk densities better observational uncertainties lead to better determination of the core and atmosphere masses, respectively. We find an intermediate regime which is completely dominated by the degeneracy.

Adding stellar abundances as a proxy for the planet

We find that using the stellar Fe/Si and Mg/Si abundances as a proxy for the bulk planetary abundances does not always provide more information on the internal parameters, it depends on the measured stellar abundances. More details coming soon in a future paper.

Research founded by

PlanetS

jonfr17@gmail.com